



Fayalitic slag as a secondary raw material for sustainable solar heat absorber and storage media

Dorothea Schneider¹, Gözde Alkan², Peter Mechich², Bernd Friedrich¹

¹ RWTH Aachen University, IME Process Metallurgy and Metal Recycling, Intzestraße 3 52056 Aachen, Germany

² DLR Cologne, Institute of Materials Research, Linder Höhe 51147 Cologne, Germany

dschneider@ime-aachen.de, Gözde.Alan@dlr.de, Peter.Mechich@dlr.de, bfriedrich@ime-aachen.de

Keywords: Concentrated Solar Power (CSP); ceramic particles; fayalitic slag; alumina; doting; by-product; thermal energy storage (TES) systems

Abstract

There is a growing demand for energy that is as sustainable and resource-efficient as possible increases. That is why Concentrated Solar Power (CSP) technology has become a focus of research. High temperature resistant ceramic particles are promising solar heat absorbers and storage media due to their high conversion coefficient and storage density. Therefore, in this approach fayalitic oxide residues will be modified and used as high temperature resistant ceramic particles and a scientific methodology to create a solar heat absorber and storage media with fayalitic by-products as oxidic residues. Since there are a large number of parameters and their potential interactions, a systematic analysis is required to understand and control the melting and post-melting thermal treatment processes. Initially, the fayalitic by-product was statistically analysed for batch-to-batch reproducibility. Based on these results, initial trials with fayalitic slag were carried out. The engineering of fayalitic slag focuses on doting, melting and cooling strategies. The different doting and cooling strategies being systematically varied in laboratory scale trials to understand and maximise crystallisation in the fayalitic system. The first step was to identify promising cooling rates and to compare different fayalitic slags with different residue components from previous industrial processing. In this study, the fayalitic slag will be developed using previous results as a basis for modification by adding doting agents from ceramic residues for targeted reaction control mechanisms. This work focusses on doting the fayalitic slag with alumina. The doting will have the aim to create more specific thermal, optical and structural properties for the heat storage medium.

Introduction

Sustainable and resource-efficient energy production has increasingly come into focus in recent years. This is one of the reasons why concentrated solar power (CSP) and thermal energy storage (TES) systems are being further researched as sustainable energy production options using solar energy.¹



One further advantage of those systems is that TES allows heat storage and resulting with that energy generation even when the sun is not shining.² Currently, a salt mixture is used to capture, transport and store heat as a heat absorber and storage medium. To identify a more environmentally friendly solar heat absorber and storage medium with improved properties and greater efficiency than the currently used salt mixtures, several approaches are currently under research.^{3,4} The main focus is on the following properties required for a suitable solar heat absorber and storage medium: high heat capacity, excellent wear resistance, long-term durability, and effective solar absorptivity.^{5,6} As a result, the focus of research has shifted to the modification and utilisation of oxide residues as high-temperature resistant ceramic particles for solar heat absorbers and storage media.^{1,2}

This study investigates the engineering of fayalitic slag as a secondary residue, focusing on doping with alumina and cooling strategies. The overarching aim is to produce a material with high crystallinity, a high heat capacity, temperature stability up to 1000 °C and good abrasion resistance.^{1,2,5} Therefore, to understand and maximise crystallisation in the fayalitic system, different cooling and alumina doping strategies are combined and systematically varied in laboratory-scale experiments.

Materials and Methods

The investigations in this study are conducted using fayalitic slag aligned with the copper route. The slag is produced synthetically at IME Aachen. To facilitate further trials and ensure homogeneity, the slag was granulated using a water quenching method. The composition of the slag, with a focus on the primary components, is presented in Table 1 and was measured using an X-ray fluorescence spectrometer (XRF, PANalytical WDXRF spectrometer Axios).

Table 1: Composition of the synthetic fayalitic slag

Compound	Na ₂ O	MgO	Al ₂ O ₃	SiO ₂	SO ₃	CaO	Fe ₂ O ₃	CuO	ZnO	PbO
wt. %	0.37	1.49	3.20	26.26	0.86	2.69	62.48	1.44	0.89	0.33

The trials are conducted in a resistance-heated chamber furnace. The material is introduced into a 0.2 l alumina crucible, using 200 g of with alumina doped slag for each trial. The furnace is heated at a rate of 250 °C/h up to 1200 °C, which is maintained for 2 hours to ensure that the entire slag is melted and homogenised within the crucible. The entire process is carried out under an argon atmosphere, with a flow rate of 1 l/min supplied to the resistance-heated furnace. Various cooling strategies and different amounts of doping alumina are tested. The cooling rates were previously investigated in a study with undoped slags⁷. The most promising cooling rates are taken up in this study and range from 300 °C/h down to 10 °C/h, while the tested amount of doping the fayalitic slag will vary between 1 to 10 wt. % of alumina. The alumina (Almatis CT 9 G) has a purity of 99.5%, with trace amounts of impurities including potassium, iron oxide, and silicon oxide. Figure 1 shows an example of a crucible cut in half after a test with 10% alumina, 10°C/h cooling.



Figure 1: crucible cut in half after a test with 10% alumina, 10°C/h cooling

Microstructural and chemical analyses of embedded and coated cross-sections are conducted using scanning electron microscopy (SEM Ultra 55, Zeiss, Wetzlar, Germany) and energy dispersive spectroscopy (EDX; UltiMate, Oxford, Abingdon, United Kingdom). For the cross-sectional analysis, samples are embedded in commercial epoxy resin. The phase components are examined using X-ray powder diffraction (XRD; D8 Advance, Bruker AXS, Karlsruhe, Germany). Measurements were performed with a diffractometer configured for Cu-K α radiation, focusing on 2 θ values between 10° and 80°.

Results and Discussion

The trials carried out in this study aimed to investigate different cooling and alumina doting strategies, with cooling rates ranging from 300 °C/h to 10 °C/h and alumina doting levels in the fayalitic slag varying between 1 and 10 wt %. The entire process in the furnace is carried out under an argon atmosphere to prevent any possible reactions with ambient air.

Figure 2 shows the SEM images of samples from the trials carried out. Picture a) to c) shows a cooling rate of 300 °C/h, picture d) to f) a cooling rate of 10 °C/h with different doting amounts of alumina. It is noticeable that the grain size of the coarse grains increases with a reduction in the cooling rate from 300 °C (see Picture a) to c)) to 10 °C (see Picture d) to f)), regardless of the amount of doting with alumina. The not with alumina doted samples, see Figure 2 a), d) show in comparison to the doted samples (see Figure 2 picture b), c), e), f)) despite the glassy matrix and the coarse grains some needle structure. In a comparison of the two non-doped compounds, it can also be seen that the needle-like structure is much more pronounced at a cooling rate of 300 °C/h compared to the cooling rate of 10 °C/h. This can be recognised above all by a significantly increased occurrence of the needle structure as well as larger and longer needles. In the doped experiments, a glassy matrix containing large and comparatively much smaller grains can be recognised regardless of the cooling rate and doting quantity. In general, the size of the grains increases at a lower cooling rate of 10°C/h. Furthermore, it is noticeable that at higher cooling rates with aluminium (see Figure 2 Fig. c), f)) the combination of large grains in the matrix and an increased number of significantly smaller grains surrounding the large grains in the matrix can be detected.

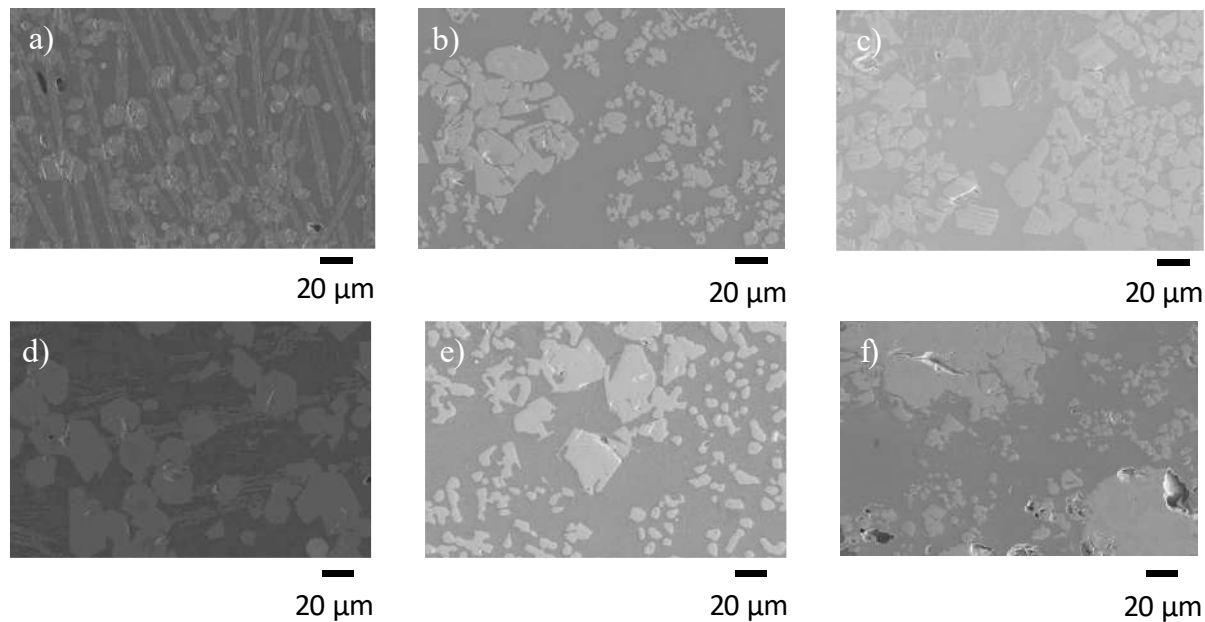


Figure 2: SEM pictures of: a) 300 °C no doting, b) 300 °C 1 wt.%, c) 300 °C 10 wt.%, d) 10 °C no doting, e) 10 °C 1 wt.%. f) 10 °C 10 wt.%

In order to identify the primary elements present in the amorphous and crystalline phases shown in Figure 2, EDX mapping (shown in Figure 3) was performed on these regions. It can be seen from the EDX mapping in Figure 3 a), e) that the needle-like structure previously detected in the undoped experiments consists mainly of iron- and silicon-oxide. Further metallic copper components coloured in pink can be detected in Figure 3 a), e) at the not doted samples. The coarse grains are coloured greenish in the EDX mapping of the undoped samples, whereby it is noticeable that the grains in image d) are coloured darker than in image a). The pure green colouring corresponds to the element alumina. In the undoped sample in Figure a), the grains contain iron and magnesium oxide as well as alumina. The undoped sample in Figure d) contains only iron oxide in addition to alumina.

The samples doped with alumina (see Figure 3 b), c), e), f)) have a matrix rich in magnesia, alumina and iron oxide. The grains in the matrix are lighter in colour than the matrix. This indicates that the yellow-coloured iron oxide has accumulated there. With higher amounts of alumina doting (see Figure 3 c), f)) the amount of turquoise coloured alumina areas increases independent of the cooling rate. The alumina accumulates in and around the large grains. This is particularly noticeable at a cooling rate of 300°C/h in Figure c)).

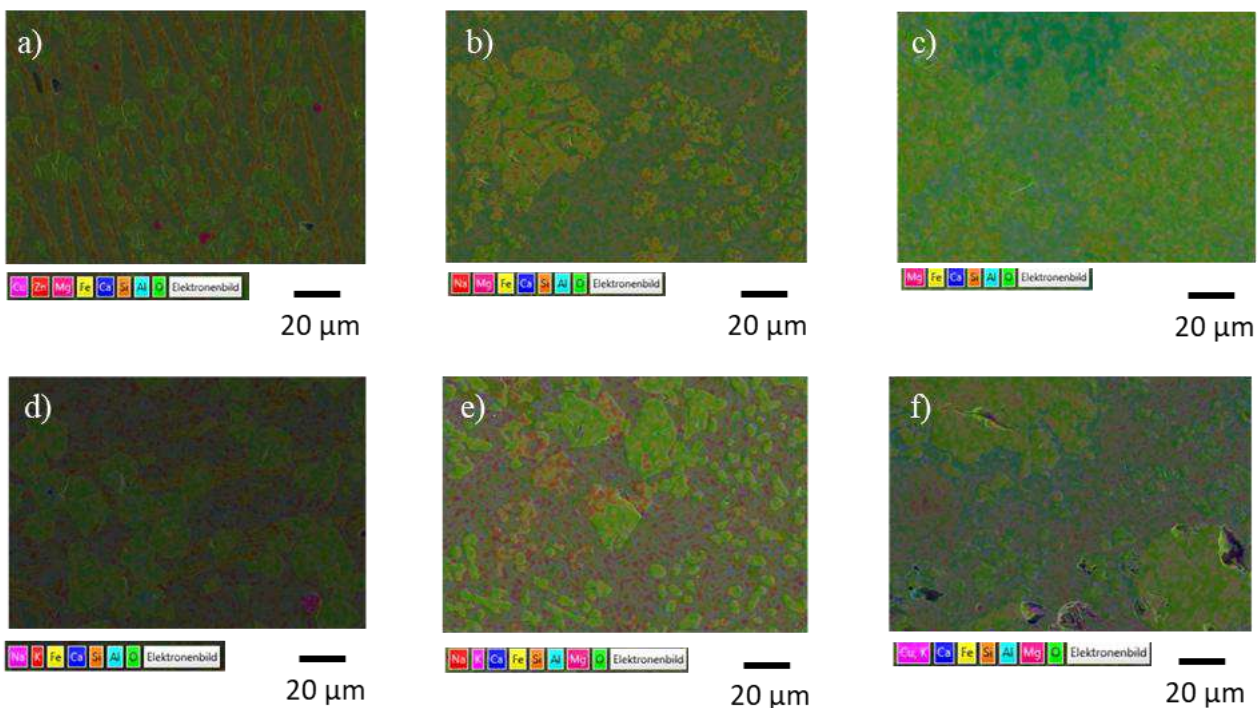


Figure 3: EDX Mapping of: a) 300 °C no doting, b) 300 °C 1 wt.%, c) 300 °C 10 wt.%, d) 10 °C no doting, e) 10 °C 1 wt.%. f) 10 °C 10 wt.%

To evaluate the resulting phases a XRD analysis is shown in Figure 4 and Figure 5. In validation with the EDX mappings shown in Figure 3, it is possible to draw conclusions about the phases located in the respective regions under discussion.

First, for the not doted samples it has been demonstrated that the needle-like structure detected in Figures 2 a) and e), according to EDX mapping, is rich in iron oxide and silica. In conjunction with the XRD results presented in Figures 3 and 4, it can be concluded that needle-like fayalite structures were formed during the undoped trials. Furthermore, Figure 3 a) shows that magnesia, alumina, and iron oxide were detected in the coarse grains. In conjunction with the XRD analyses presented in Figures 3 and 4, it can be concluded that the grains in the not doted sample with a cooling rate of 300 °C/h primarily contain the phases magnetite and Mg-Fe-Al spinel. In comparison, in the undoped trials at a cooling rate of 10 °C/h, iron oxide is predominantly detected in the coarse grains alongside alumina. With the aid of the XRD analysis presented in Figures 3 and 4, it can be concluded that in this sample, the grains primarily contain the phase magnetite, however, the phase hematite can also be detected.

Furthermore, for the alumina-doped trials shown in Figures 2 b), c), e), and f), magnesia, alumina, and iron oxide are detected in the matrix. According to the XRD diffractograms presented in Figures 3 and 4, this indicates that the matrix is rich in a magnesia-alumina-iron oxide spinel. Since, according to the EDX mappings in Figures 2 b), c), e), and f), the coarse grains contain more silicon oxide than the matrix, consideration of the XRD results presented in Figures 3 and 4 indicates that the grains exhibit the phase hematite. Additionally, the EDX mappings in Figures 2 c) and f) reveal that the



highest alumina doting levels correspond to 10 wt. % alumina precipitations. For the cooling rate of 300 °C/h (see Figure 4), alumina can be identified in its pure form as corundum. However, for the comparatively lower cooling rate of 10 °C/h, pure corundum can no longer be detected using XRD (see Figure 5). It appears that due to the extended cooling time, the alumina has been associated with calcium oxide and silicon oxide to form anorthite.

16

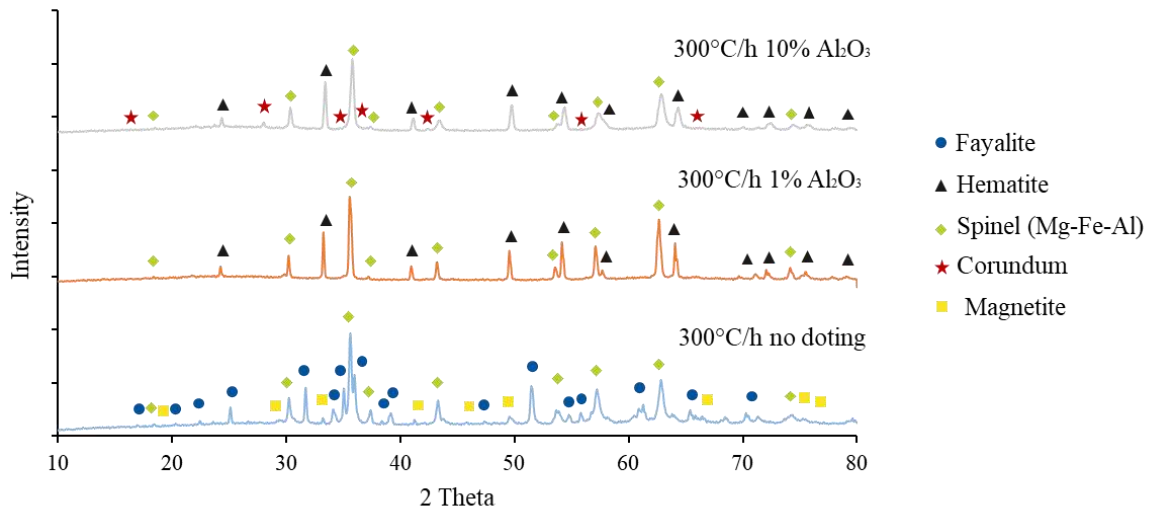


Figure 4: XRD results of the cooling rate 300 °C/h

Another significant difference between the cooling rates of 300 °C/h and 10 °C/h is that, at the slower cooling rate, additional phases such as anorthite and cristobalite are formed (see Figure 5). It is noteworthy that the formation of anorthite can only be detected in the trial with 10 wt. % doting. The precipitation and formation of additional aluminium oxide phases could be observed at the lower doting level of 1 wt. %.

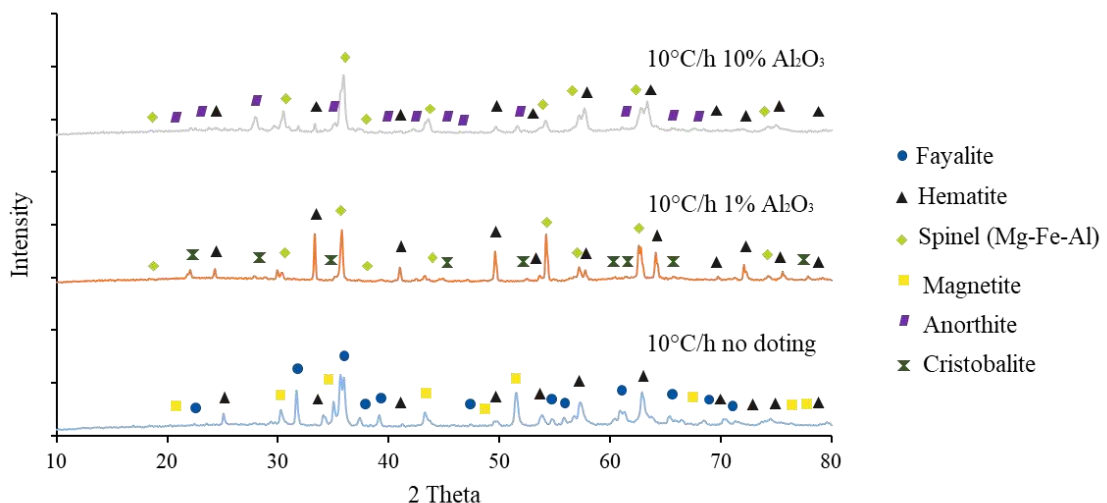


Figure 5: XRD results of the cooling rate 10 °C/h



Furthermore, it is demonstrated that the formation of hematite can be induced through alumina doting even at faster cooling rates of 300 °C/h (see Figure 4 and Figure 5). Furthermore, it can be observed that at higher doting levels of 10 wt. % alumina, corundum precipitations form at the cooling rate of 300 °C/h (see Figure 3 c) and Figure 4). At the lower cooling rate of 10 °C/h, the alumina at the higher doting levels of 10 wt. % interacts with other components of the system, leading to the formation of the phase anorthite (see Figure 3 f) and Figure 5).

Conclusion

The engineering of fayalitic slag is achieved by emphasising doting and cooling strategies. Systematic variations of different doting and cooling approaches are conducted through laboratory-scale trials to enhance and maximise crystallisation within the fayalitic system. The properties in focus to achieve a new material as a solar heat absorber and storage medium are: high heat capacity, excellent wear resistance, long-term durability, and effective solar absorptivity.^{5,6} Systematic variations of different doting and cooling approaches are conducted in this study through laboratory-scale trials to enhance and maximise crystallisation within the fayalitic system. The results indicate that lower cooling rates lead to increased crystallinity, facilitating the formation of more stable iron-rich phases, particularly in the transition from fayalite to magnetite and ultimately to haematite. Furthermore, previous studies by Alkan et al.^{1,2} have shown that the phases characterised by reduced amorphous content and increased crystallinity are advantageous for use as ceramic particles in solar heat absorbers and storage media. The observed increase correlates with improved wear resistance of the particles within the CSP plant, highlighting their potential utility in this context.

In conclusion, the investigation into both undoped and alumina-doped fayalitic slag has provided valuable insights into the crystallisation behaviour and phase formation under varying cooling rates. For the undoped samples, it was demonstrated that the needle-like structures identified are rich in iron oxide and silica, with XRD analyses confirming the presence of needle-like fayalite structures. The coarse grains were found to primarily contain magnetite and Mg-Fe-Al spinel at a cooling rate of 300 °C/h, while at a slower cooling rate of 10 °C/h, these grains predominantly exhibited magnetite along with detectable hematite.

In the alumina-doped trials, significant findings included the detection of magnesia, alumina, and iron oxide within the matrix, indicating a composition rich in magnesia-alumina-iron oxide spinel. The coarse grains contained higher amounts of silicon oxide compared to the matrix, suggesting their association with hematite. Notably, higher doping levels (10 wt. %) led to pure corundum formation at a cooling rate of 300 °C/h; however, this was not observed at a lower cooling rate due to interactions leading to anorthite formation.

The study further highlighted that additional phases such as anorthite and cristobalite emerged at slower cooling rates. Importantly, the precipitation of further aluminium oxide phases was noted even at lower doping levels (1 wt. %). One important point in this study is that the formation of hematite



can be induced through alumina doping even at faster cooling rates of 300 °C/h, in contrast to undoped samples, where hematite formation was only observed at slower cooling rates.

These findings contribute to our understanding of how varying doping and cooling strategies can influence phase stability and material properties in fayalitic slag systems for potential applications in solar heat absorption and storage media.

In further research will focus on improving the properties essential for CSP applications, including excellent wear resistance, long-term durability, high heat capacity, and effective solar absorptivity^{5,6}. The aim will be to investigate a wider range of cooling rates to further develop the fayalitic slag as a base material for subsequent modifications^{1,8}. In future studies, the targeted control of reactions through the addition of doting agents will be modelled using FactSageTM^{9,10} calculations and then investigated in laboratory-scale experiments. The implementation of further oxides as doting agents has the effect of refining the crystallization process and optimising the products, thereby improving the functional properties required for use as solar heat absorbers and storage media for CSP technology^{1,2}.

Acknowledgements

The authors acknowledge that the “Engineering of tailored secondary oxide raw materials for sustainable solar heat absorber and storage media” Project is founded by the Deutsche Forschungsgemeinschaft (DFG, German Research Foundation) - 528382263.

References

1. Alkan G, Mechnich P, Lucas H, et al. Assessment of Metallurgical Slags as Solar Heat Absorber Particles. *Minerals*. 2022;12(2):121.
2. Alkan G, Mechnich P, Barbri H, et al. Evaluation of ceramic proppants as heat transfer and storage medium. In: *THE INTERNATIONAL CONFERENCE ON BATTERY FOR RENEWABLE ENERGY AND ELECTRIC VEHICLES (ICB-REV) 2022*: AIP Publishing; 2023:160002.
3. Buck R, Giuliano S. Solar tower system temperature range optimization for reduced LCOE. In: *SOLARPACES 2018: International Conference on Concentrating Solar Power and Chemical Energy Systems*: AIP Publishing; 2019:30010.
4. Ortega-Fernández I, Calvet N, Gil A, Rodríguez-Aseguinolaza J, Faik A, D'Aguanno B. Thermophysical characterization of a by-product from the steel industry to be used as a sustainable and low-cost thermal energy storage material. *Energy*. 2015;89:601–609.



5. Calderón A, Barreneche C, Palacios A, et al. Review of solid particle materials for heat transfer fluid and thermal energy storage in solar thermal power plants. *Energy Storage*. 2019;1(4).
6. Alkan G, Mechnich P, Pernpeintner J. Using an Al-Incorporated Deep Black Pigment Coating to Enhance the Solar Absorptance of Iron Oxide-Rich Particles. *Coatings*. 2023;13(11):1925.
7. Dorothea Schneider, Gözde Alkan, Peter Mechnich, Bernd Friedrich. Study on slag design of fayalitic by-products as an oxide raw material for solar heat absorber and storage media. *proceeding: 9th international slag valorisation symposium*. 2025.
8. X.Wang, D.Geysen, S.V. Padilla T., N.d'Hoker, T. Van Greven, B. Blanpain. Characterization of copper slag. 2013.
9. Bale CW, Béliste E, Chartrand P, et al. FactSage thermochemical software and databases, 2010–2016. *Calphad*. 2016;54:35–53.
10. Hugo Lucas, Joao Pedro Weiss, Bernd Friedrich. "Modelling pyrometallurgical systems through oxygen partial pressure to fit experimental data" Study case: fayalitic slags GTT Users' Meeting 2024; 2024.